

String Method for Generalized Gradient Flows: Computation of Rare Events in Reversible Stochastic Processes

Tobias Grafke

Mathematics Institute, University of Warwick, Coventry CV4 7AL, United Kingdom*



~~Abstract~~
~~up to 1000 characters~~
~~should be provided~~
~~for the arXiv preprint~~
~~archive~~
~~at the time of submission~~
~~of the paper~~
~~to the arXiv preprint~~
~~archive~~

I. INTRODUCTION

Meta-stability frequently occurs in nature. A complex stochastic dynamical system often has multiple locally stable fixed points close to which it spends the majority of its time. Rarely, and on a much longer time-scale, fluctuations push the system from one such state to another. Typical examples include chemical reactions under thermal noise [1], nucleation [2], crystal deformation [3], etc. Another common setup is the coarse-graining of microscopic models in statistical mechanics, where effective dynamics can be derived including noise terms as fluctuating hydrodynamics [4]. If the effective limiting dynamics have multiple fixed points, such as for phase transitions, or when conditioning on rare observables, the intrinsic stochastic noise induced by the finiteness of the number of particles will trigger the rare event, a situation that is quantified by *macroscopic fluctuation theory* [5].

In all these cases, the computation of the most likely transition pathway is practically achievable if a *large deviation principle* (LDP) holds [6]. Whenever present, the LDP demands that the least unlikely of all transition scenarios will exponentially dominate all others, reducing the original stochastic sampling problem to a deterministic optimization problem. The analytical computation of the corresponding minimizers (*maximum likelihood pathways*, MLPs) is often impossible, and their numerical computation leads to a high-dimensional optimization problem, which for systems with a large number of degrees of freedom is hard to solve. The computation of the MLP is significantly simplified for a specific subclass of stochastic processes: Whenever the dynamics is a diffusion in a potential landscape with small noise, the invariant measure of the process is explicitly known from the potential itself, and MLPs become minimum energy paths. The computation of transition trajectories is then simplified to the computation of heteroclinic orbits of the gradient flow, which is numerically achieved by the string method [7, 8].

An evolution driven by a negative gradient of a potential is a straightforward example of a gradient flow. Recent breakthroughs allowed phrasing many more reversible systems as (generalized) gradient flows, starting with recognizing the Wasserstein gradient structure of the Fokker-Planck equation of Itô stochastic differential equations (SDEs) [9]. The relation to large deviation principles of microscopic particle systems is by now well understood [10]. The resulting class of dynamics is no longer restricted to diffusions or even the Gaussian case, but applicable e.g. to jump processes, lattice gas models or interacting particle systems. The main point of this paper is to show that under certain conditions, transition trajectories in reversible stochastic processes are heteroclinic orbits (or their time-reverse) of the associated generalized gradient flow. This allows us to derive a generalized string method for the efficient and robust computation of the MLPs.

II. MAIN RESULTS

Let $X_t^\varepsilon \in \mathcal{E}^\varepsilon$ be a family of continuous time Markov jump processes (MJPs) in the state spaces \mathcal{E}^ε . If X_t^ε

- (i) fulfills a pathwise LDP in the limit $\varepsilon \rightarrow 0$ with rate function

$$I_T(\phi) = \int_0^T L(\phi, \dot{\phi}) dt$$

for *Lagrangian* L , and corresponding *Hamiltonian* H given by the Fenchel-Legendre transform

$$H(\psi, \theta) = \sup_{\eta} (\langle \theta, \eta \rangle - L(\psi, \eta)) ,$$

and

- (ii) obeys detailed balance,

then the transition trajectory $\{\phi(\tau)\}$ between two fixed points a and b in the limit $\varepsilon \rightarrow 0$ fulfills

$$\dot{\phi} = -\partial_\theta H(\phi, 0)$$

* T.Grafke@warwick.ac.uk

between a and the ‘‘relevant saddle’’ z , and

$$\dot{\phi} = \partial_{\theta} H(\phi, 0)$$

between z and b . In particular, the transition trajectory, i.e. the trajectory $\phi(t)$ and corresponding T that minimize $I_T(\phi)$, is described by the heteroclinic orbits (and their time-reverse) of the *generalized gradient flow* field $\partial_{\theta} H(\phi, 0)$. This includes the previously known case of diffusions in a potential $U(\phi)$, where $\dot{\phi} = \pm \nabla U(\phi)$.

The main result of the paper is that we can then numerically compute the transition trajectory with the *generalized string method*, which, starting from an initial guess ϕ_i^0 , where $i \in \{1, \dots, N\}$ enumerates system copies along the trajectory, iterates only two simple steps until convergence:

- (i) Update to temporary states $\tilde{\phi}_i$,

$$\tilde{\phi}_i = \phi_i^k + \Delta t \partial_{\theta} H(\phi_i^k, 0).$$

- (ii) Reparametrize $\tilde{\phi}_i$ to obtain next iterates ϕ_i^{k+1} that fulfill,

$$\|\phi_{i+1}^{k+1} - \phi_i^{k+1}\| = \text{cst.} \quad \forall i \in \{1, \dots, N\}.$$

The knowledge of the transition trajectory yields not only information about the most likely transition in the large deviation limit, but furthermore allows one to estimate the exponential scaling of its probability. Additionally, it yields the relevant saddle point (transition state) of the limiting dynamics, i.e. the points where the trajectory crosses the separatrix between one basin of attraction and another, and can be used as a ‘reaction coordinate’ as a basis for more sophisticated sampling techniques, such as forward flux sampling [11], cloning or splitting algorithms [12–14] or importance sampling.

In what follows, we will first derive the main results of the paper in section III. Subsequently, in section IV, the connection to the mathematical literature on generalized gradient flows is made. In section V, the numerical computation of limiting trajectories is discussed, and the full string method for generalized gradient flows is introduced. Finally, its capabilities are demonstrated in section VI on several examples, including a bi-stable reaction network, a zero range lattice gas model exhibiting condensation, and the hydrodynamic limit of interacting particles.

III. TRANSITION TRAJECTORIES IN REVERSIBLE MARKOV JUMP PROCESSES

A. Large deviation principles and transition trajectories

Let $X_t^{\varepsilon} \in \mathcal{E}^{\varepsilon}$ be a family MJP in the state spaces $\mathcal{E}^{\varepsilon}$ with generators $\mathcal{L}^{\varepsilon}$ and unique invariant measures $\mu_{\infty}^{\varepsilon}$.

We say that X_t^{ε} fulfills a pathwise *large deviation principle* (LDP) if, for $\delta > 0$ sufficiently small, the probability to observe a sample path close to a given trajectory $\phi(t)$ fulfills

$$\mathcal{P}(\sup_{t \in [0, T]} |X_t^{\varepsilon} - \phi(t)| < \delta) \asymp \exp(-\varepsilon^{-1} I_T(\psi)). \quad (1)$$

Here, the sign \asymp stands for asymptotic logarithmic equivalence, i.e. that for $\varepsilon \rightarrow 0$, the logarithm of both sides has the same limit, and

$$I_T(\psi) = \int_0^T L(\psi, \dot{\psi}) dt.$$

The quantity $L(\psi, \dot{\psi})$ is called the *Lagrangian*, which admits a corresponding *Hamiltonian* as its Fenchel-Legendre transform

$$H(\psi, \theta) = \sup_{\eta} (\langle \theta, \eta \rangle - L(\psi, \eta)).$$

The probability to observe a transition starting in a neighborhood of a point $a \in \mathcal{E}$ to a neighborhood of a point $b \in \mathcal{E}$ can be obtained by a minimization over suitable trajectories ψ ,

$$\mathcal{P}(a \rightarrow b) \asymp \exp(-\varepsilon^{-1} \inf_{\psi \in \mathcal{C}_a^b} I_T(\psi)) \quad (2)$$

with $\mathcal{C}_a^b = \{\psi(t) \in \mathcal{D}[0, T] | \psi(0) = a, \psi(T) = b\}$, \mathcal{E} denoting the limiting state space, and $\mathcal{D}[0, T]$ the Skorokhod space on $[0, T]$. For a precise definition of large deviation principles for stochastic processes, see e.g. [15]. In the course of this paper, we are interested in finding explicitly the *minimizer* (or *instanton*) ϕ that solves the minimization problem (2) for given endpoints a, b ,

$$I_T(\phi) = \inf_{\psi \in \mathcal{C}_a^b} I_T(\psi),$$

when additionally minimizing over the transition time T . This minimizer $(\phi(t), T)$ describes the most likely transition trajectory in the limit $\varepsilon \rightarrow 0$. It can equivalently be described as a solution to the Hamilton’s equations

$$\dot{\phi} = \partial_{\theta} H(\phi, \theta), \quad \dot{\theta} = -\partial_{\phi} H(\phi, \theta). \quad (3)$$

A special case is the situation of a trajectory $\phi(t)$, such that $I_T(\phi) = 0$. Since $L \geq 0$, these trajectories are necessarily (global) minimizers, and are called *zero action pathways* or *relaxation dynamics*. The equivalent dynamics define a *deterministic* dynamical system as limit of the original stochastic process which can be interpreted as a law of large numbers (LLN) or hydrodynamic limit of the MJP. In terms of the Hamiltonian, they correspond to solutions of (3) with $\theta = 0, \dot{\theta} = 0$, and therefore

$$\dot{\phi} = \partial_{\theta} H(\phi, 0).$$

In the situation where the relaxation dynamics have a unique and stable fixed point a , i.e. $\partial_{\theta} H(a, 0) = 0$, and we

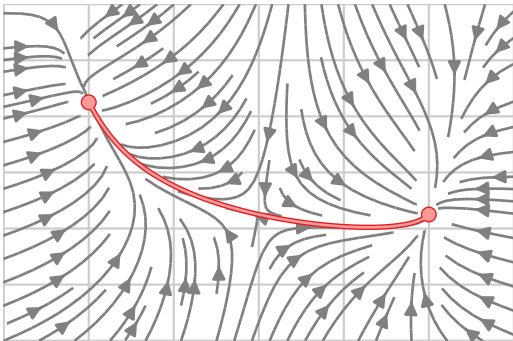


Figure 1: A phase space plot showing a vector field of trajectories. Two fixed points are marked with red dots. A red trajectory connects the two fixed points, representing a transition path. The trajectories are grey arrows, and the red trajectory is a smooth curve connecting the two fixed points.

$$\dot{\phi} = \partial_{\theta} H(\phi, \theta)$$

only consider trajectories starting from that fixed point, we can define the *quasipotential* $V(x)$ by

$$V(x) = \inf_{T>0} \inf_{\phi \in \mathcal{C}_a^x} I_T(\phi). \quad (4)$$

The quasipotential loosely quantifies the difficulty of reaching a point x via the stochastic process and generalizes the notion of a free energy to non-equilibrium systems. It is connected to the invariant measure $\mu_{\infty}^{\varepsilon}$ of the MJP through the relation $\lim_{\varepsilon \rightarrow 0} \varepsilon \log \mu_{\infty}^{\varepsilon}(A) = -\inf_{x \in A} V(x)$ (see [6, Chpt 4, Thm 4.3] for details).

For transition trajectories between two fixed points a and b , as depicted in figure 1, we realize that the definition of the quasipotential (4) holds true locally in each basin of attraction. A restriction of the arguments to single basins, and subsequent ‘stitching’ of $V(x)$ to neighboring basins [16], proves to be sufficient to describe bistable transitions of the form of figure 1, as we will see in the next section.

B. Adjoint Process and Reversibility

For a reversible MJP $X_t \in \mathcal{E}$, the *adjoint process*, generated by the $L^2(\mathcal{E}, \mu_{\infty})$ -adjoint of \mathcal{L} is equal to the process itself, i.e. for ρ_{∞} being the density of μ_{∞} with respect to counting or Lebesgue measure,

$$\mathcal{L} = \rho_{\infty}^{-1} \mathcal{L}^{\dagger} \rho_{\infty},$$

where \mathcal{L}^{\dagger} is the usual $L^2(\mathcal{E})$ -adjoint of \mathcal{L} . Intuitively, the probability of starting at a and observing the trajectory $\psi(t)$ is equal to the probability of observing the reverse trajectory $\psi^*(t) = \psi(T-t)$ starting at b . For a family of reversible MJPs $(X_t)^{\varepsilon}$, with LDT Lagrangian L and Hamiltonian H , this can be expressed as

$$V(a) + \int_0^T L(\psi, \dot{\psi}) dt = V(b) + \int_0^T L(\psi, -\dot{\psi}) dt, \quad (5)$$

for any trajectory $\{\psi\}_{t \in [0, T]}$ with $\psi(0) = a, \psi(T) = b$ (compare [10, Thm 3.3]).

Written in terms of the Hamiltonian, this translates to

$$H(\psi, \theta) = H(\psi, \nabla V - \theta). \quad (6)$$

This is a consequence of (5), which implies

$$L(\psi, \dot{\psi}) = L(\psi, -\dot{\psi}) + \frac{d}{dt} V(\psi) = L(\psi, -\dot{\psi}) + \langle \nabla V, \dot{\psi} \rangle \quad (7)$$

and therefore

$$\begin{aligned} H(\psi, \theta) &= \sup_{\eta} (\langle \eta, \theta \rangle - L(\psi, \eta)) \\ &= \sup_{\eta} (\langle \eta, \theta \rangle - \langle \eta, \nabla V \rangle - L(\psi, -\eta)) \\ &= \sup_{-\eta} (\langle \eta, \nabla V - \theta \rangle - L(\psi, \eta)) \\ &= H(\psi, \nabla V - \theta). \end{aligned}$$

Defining an entropy function $S(x) = 2V(x)$, this equation can be rewritten [10, Prop 2.1] as

$$H(\psi, \nabla S - \theta) = H(\psi, \nabla S + \theta). \quad (8)$$

C. Minimizing Trajectories of the Action of Reversible Processes

We now want to focus on the minimizing trajectories of the action for reversible processes, i.e. the solutions (ϕ, T) to the minimization problem (4) under the assumption that the process is reversible.

Consider first the case that we start at a point a that is a fixed point of the limiting dynamics, i.e. $\partial_{\theta} H(a, 0) = 0$. We want to investigate the minimizing transition trajectory to a point b within the same basin of attraction. Denote by (ϕ, T) the minimizing pair for the quasipotential, equation (4). Since a is a fixed point, this necessitates $V(a) = 0$ and $T = \infty$. Then, equation (4) becomes $V(b) = \int_0^{\infty} L(\phi, \dot{\phi}) dt$. By plugging this into equation (5), this shows that $\phi(t)$ is also a trajectory that has

$$L(\phi, -\dot{\phi}) = 0. \quad (9)$$

In other words, minimizers originating at the fixed point are time-reversed relaxation trajectories. More precisely, combining equations (7) and (9), we have

$$L(\phi, \dot{\phi}) = \langle \nabla V(\phi), \dot{\phi} \rangle \quad (10)$$

and therefore $\theta = \frac{\partial L}{\partial \dot{\phi}} = \nabla V = 2\nabla S$. For this trajectory, the equation of motion thus reads

$$\dot{\phi} = \partial_{\theta} H(\phi, \nabla V(\phi)). \quad (11)$$

On the other hand, by differentiating (6) with respect to θ , and setting $\theta = 0$, we obtain

$$\partial_{\theta} H(\phi, \nabla V(\phi)) = -\partial_{\theta} H(\phi, 0). \quad (12)$$

We therefore arrive at following the proposition:

Proposition 1. *For reversible processes, minimizers $\phi(t)$ of the large deviation rate function starting at a fixed point a of the limiting dynamics, and ending at any point b within the same basin of attraction, fulfill*

$$\dot{\phi} = -\partial_{\theta}H(\phi, 0). \quad (13)$$

Next, we want to consider the case where both initial and final points a and b are fixed points with neighboring basins of attraction that together cover the whole state space. The flow $\partial_{\theta}H(\phi, 0)$ then defines a separatrix C in a dynamical systems sense that separates the two basins of attraction a and b . This separatrix possibly contains multiple saddle points z_i with $\partial_{\theta}H(z_i, 0) = 0$. Denote by z the *relevant saddle point*, i.e. the point on the separatrix which attains the minimal quasipotential, $V(z) \leq V(x) \forall x \in C$. This point necessarily is also the point through which the most likely transition between a and b traverses from one basin of attraction to the other: A transition from a to b must leave the basin of attraction of a , which must happen at z since z minimizes the quasipotential on C . The remaining portion between z and b on the other hand can be achieved with zero cost: Since z is on the separatrix, there exists a relaxation trajectory from z to b , i.e. a trajectory ϕ connecting z and b such that

$$\dot{\phi} = \partial_{\theta}H(\phi, 0). \quad (14)$$

Alluding to the case of a diffusion in a potential, this portion of the trajectory is often called the *downhill* portion, as it coincides in this case with the direction of maximally decreasing potential. On the other hand, for the portion between a and z , proposition 1 applies, i.e. here

$$\dot{\phi} = -\partial_{\theta}H(\phi, 0). \quad (15)$$

With the same intuition, we call this portion of the trajectory the *uphill* portion, as the dynamics occur along directions of maximally increasing potential in the case of diffusion in a potential. Note though that this intuition breaks down for general reversible processes. In particular, even though the notion of the quasipotential replaces the potential, it is not true that relaxation paths are obeying $\dot{\phi} = -\nabla V(\phi)$. Instead, relaxation paths are *generalized gradient flows* in the quasipotential, and uphill paths are time reversed *generalized gradient flows* in the quasipotential. Both are not necessarily aligned with the direction of maximal increase or decrease of the quasipotential.

For the complete transition trajectory, we therefore have, under the above assumptions (a and b being neighboring fixed points, with basin of attraction covering the complete state space):

Proposition 2. *For reversible processes, minimizers $\phi(t)$ of the large deviation rate function connecting two fixed points a and b fulfill*

$$\dot{\phi} = \partial_{\theta}H(\phi, 0) \quad (16)$$

in the uphill portion from a to the relevant saddle point z , and

$$\dot{\phi} = -\partial_{\theta}H(\phi, 0) \quad (17)$$

for the downhill portion from z to b .

Note that both up- and downhill portion of the transition trajectory are readily available by simple integration, and no reference is made to the quasipotential. This generalizes the known case of diffusions in a potential $U(\phi)$, where the minimizers of the rate function fulfill either

$$\dot{\phi} = -\nabla U(\phi) \quad \text{or} \quad \dot{\phi} = \nabla U(\phi).$$

Intuitively, proposition 2 states the unsurprising fact that time-reversal symmetry is obeyed for transition trajectories in reversible processes. At the same time, it implies that all minimizing trajectories are *heteroclinic orbits* or time-reversed heteroclinic orbits of the *generalized gradient flow* induced by the large deviation principle of X_t^{ε} . It therefore allows for an extension of the string method [7] to more general situations, which is the main contribution of this paper. This will be discussed in section V.

IV. CONNECTION TO GENERALIZED GRADIENT FLOWS

To make the connection to the mathematical literature, we want to highlight here the relation of the above considerations to generalized gradient flows and their connection to large deviation theory. This is of particular importance in the context of statistical mechanics and stochastic thermodynamics, where the connection between large deviations and hydrodynamic limits [5], statistical mechanics [17] and non-equilibrium thermodynamics [18] is known in considerable detail.

Consider the space \mathcal{E} to be a Riemannian manifold, with tangent bundle $T\mathcal{E}$ and cotangent bundle $T^*\mathcal{E}$. Define on \mathcal{E} a convex, continuously differentiable function $\psi_x(v) : T\mathcal{E} \rightarrow \mathbb{R}^+$ and its Legendre-dual $\psi_x^*(w) : T^*\mathcal{E} \rightarrow \mathbb{R}^+$,

$$\begin{aligned} \psi_x^*(w) &= \sup_{v \in T_x \mathcal{E}} (\langle v, w \rangle - \psi_x(v)) \\ \psi_x(v) &= \sup_{w \in T_x^* \mathcal{E}} (\langle v, w \rangle - \psi_x^*(w)). \end{aligned}$$

Additionally we demand $\psi_x(0) = \psi_x^*(0) = 0$. Then, (ψ, ψ^*) are called *dissipation potentials* in the context of thermodynamics.

Furthermore, consider a continuously differentiable function $S : \mathcal{E} \rightarrow \mathbb{R}$. Then, any evolution on \mathcal{E} according to $\dot{x} = F(x)$ that fulfills

$$\psi_x(F(x)) + \psi_x^*(-\nabla S(x)) + \langle F(x), \nabla S(x) \rangle = 0$$

is called a *generalized gradient flow* with respect to (\mathcal{E}, ψ, S) [10]. This is equivalent to saying

$$\dot{x} = \partial_w \psi_x^*(-\nabla S(x)). \quad (18)$$

In the case of a gradient diffusion, the dissipation potential $\psi_x^*(w)$ is quadratic in w (the quadratic dependence being a consequence of the Gaussianity of the noise, the metric implied by its covariance). In that case, $\partial_w \psi_x^*(w)$ is linear in its argument, and thus the flow (18) is a traditional gradient flow proportional to $\nabla S(x)$. Allowing for generic dissipation potentials $\psi_x^*(w)$ explains why the flows (18) are called *generalized* gradient flows.

The connection to large deviations is made when taking

$$\psi_x^*(\theta) = H(x, \theta + \nabla S(x)) - H(x, \nabla S(x)), \quad (19)$$

for a large deviation Hamiltonian $H(\psi, \theta)$ of a reversible process. The choice (19) fulfills the assumptions of (ψ, ψ^*) to be dissipation potentials, and a gradient flow can be constructed out of the large deviation principle, or, equivalently, the optimization problem of large deviations can be interpreted as the variational formulation of a generalized gradient flow.

Finally, equation (18) with the choice (19), leads to

$$\dot{x} = \partial_\theta H(x, 0)$$

as gradient flow. As we will see in the examples in section VI, non-Gaussian stochastic processes lead to Hamiltonians that are not quadratic in their conjugate momentum, and therefore to generalized instead of traditional gradient flows.

V. NUMERICAL COMPUTATION OF THE TRANSITION TRAJECTORY

With the realization of proposition 2, implementing a string method for generalized gradient flows in the spirit of the original string method [7, 8] becomes straightforward.

Consider a reversible MJP $X_t^\varepsilon \in \mathcal{E}^\varepsilon$ with limiting state space \mathcal{E} that obeys a LDP with Lagrangian L and Hamiltonian H . Following [8], denote by $\phi(\tau)$, $\tau \in [0, 1]$ a *string*, i.e. a candidate limiting transition trajectory connecting two fixed points $a, b \in \mathcal{E}$. A heteroclinic orbit of the flow $\partial_\theta H(\phi, 0)$ then obeys the relations

$$\phi(0) = a, \quad \phi(1) = b, \quad (\partial_\theta H(\phi(\tau), 0))^\perp = 0, \quad (20)$$

where for a vector field $v(\phi(\tau))$ along the string $\phi(\tau)$, the notation v^\perp describes the component in the plane perpendicular to the string,

$$\begin{aligned} v(\phi(\tau))^\perp &= v(\phi(\tau)) - \langle v(\phi(\tau)), \gamma(\tau) \rangle \gamma(\tau), \\ \gamma(\tau) &= |\dot{\phi}(\tau)|^{-1} \dot{\phi}(\tau), \end{aligned}$$

and $\gamma(\tau)$ corresponds to the unit tangent vector along ϕ . Denote by ϕ_n^k , $n \in \{1, \dots, N\}$, the k -th approximation of the n -th image along the discretized string. One iteration, then consists of two steps.

- (i) Following proposition 2, integrate the forward gradient flow (16), $\dot{\phi}(\tau) = \partial_\theta H(\phi(\tau), 0)$ for every image along the string via an appropriate integration scheme. For example, when choosing forward Euler, set the temporary result

$$\tilde{\phi}_n = \phi_n^k + \Delta t \partial_\theta H(\phi_n^k, 0). \quad (21)$$

More sophisticated and higher order time integration schemes are similarly viable, including implicit ones. In particular, if the operator with the tightest stability restrictions is linear, it is generally a good idea to consider exponential time-differencing schemes [19]. In general, all considerations that are valid for the integration of the limiting dynamics also apply to the string update step. After applying (21), the images along the string are no longer distributed in an equidistant way, and would accumulate at the fixed points a or b if (21) would be repeated indefinitely. Therefore, as a second step,

- (ii) obtain the next iterate ϕ_n^{k+1} by reparametrization of $\tilde{\phi}_n$ by arc-length. The arc-length parameter of the n -th image is given by the recursive relation

$$s_0 = 0, \quad s_n = s_{n-1} + \|\tilde{\phi}_n - \tilde{\phi}_{n-1}\|.$$

This information can then be used to re-interpolate the images $\tilde{\phi}_n$ to ϕ_n^{k+1} at the positions

$$\tilde{s}_n = ns_N/N.$$

This ensures that now

$$\|\phi_{n+1}^{k+1} - \phi_n^{k+1}\| = \text{cst}.$$

The re-parametrization step moves points only along the string $\phi(\tau)$ (up to the accuracy prescribed by the interpolation scheme). Therefore, after convergence of the algorithm, the remaining change that occurs in step (i), is necessarily parallel to the string, or in other words, at the fixed point of the iteration the orthogonality condition (20) is fulfilled.

Remark 1. All results regarding computational complexity and order of convergence of the original ‘simplified and improved string method’ [8] apply also here.

Remark 2. The implementation difficulty of the string method is roughly equal to that of the limiting dynamics. Furthermore, we can solve the minimization problem with the computational cost of the forward integration of the equation, multiplied by the number of copies N . This is in stark contrast to the full optimization problem (2) posed by minimizing the original rate function, as the corresponding Euler-Lagrange equation is second order (in time), the highest order operator of which will be the original order squared. For example, if the stochastic PDE in question was the stochastic heat equation,

$$\dot{\rho} = \partial_x^2 \rho + \eta, \quad \mathbb{E}(\eta\eta') = \delta(t-t')\delta(x-x'),$$

then the corresponding Lagrangian is

$$L(\rho, \dot{\rho}) = \frac{1}{2} \int |\dot{\rho} - \partial_x^2 \rho|^2 dx$$

and the Euler-Lagrange equation, to be solved with suitable boundary conditions, is

$$0 = \frac{\partial L}{\partial \rho} - \frac{d}{dt} \frac{\partial L}{\partial \dot{\rho}} = \dot{\rho} + \partial_x^4 \rho.$$

For the string method, one only needs to integrate

$$0 = \dot{\rho} - \partial_x^2 \rho.$$

Consequently, implementation simplicity and efficiency of the string method always exceeds more complex generic optimization methods such as the MAM [2] or gMAM [20, 21], and should be preferred whenever the reversibility condition holds.

VI. EXAMPLES

A. Diffusion in a gradient potential

As a reminder of the standard setup for which the string method was originally devised, consider the case of diffusion in a gradient potential. Let the configuration space $\mathcal{E}^\varepsilon = \mathbb{R}^d$, $\forall \varepsilon > 0$, and the system state $X_t \in \mathcal{E}$ evolve according to the Itô SDE

$$dX_t^\varepsilon = -\nabla U(X_t^\varepsilon) dt + \sqrt{\varepsilon} dW_t. \quad (22)$$

Then necessarily $S(x) = U(x) = \frac{1}{2}V(x)$, and from Freidlin-Wentzell theory it follows that

$$L(\psi, \dot{\psi}) = \frac{1}{2} |\dot{\psi} + \nabla U(\psi)|^2, \quad H(\psi, \theta) = -\langle \theta, \nabla U \rangle + \frac{1}{2} |\theta|^2. \quad (23)$$

It is easy to check that indeed the reversibility condition (8) is fulfilled, i.e. $H(\psi, \nabla U - \theta) = H(\psi, \nabla U + \theta)$. The minimizers therefore follows

$$\dot{\phi} = \pm \nabla U(\phi). \quad (24)$$

Numerous applications for this setup exist, most importantly for chemical systems and molecular dynamics, including Lennard-Jones clusters, clusters of water molecules, peptides [1], crystal deformations [3], and quantum mechanics/molecular mechanics simulations [22]. A straightforward and well-known generalization of the flow (22) is to choose an additional *mobility* matrix $M(x) \in \mathbb{R}^{d \times d}$ which is symmetric and divergence free (i.e. $\sum_i \partial_{x_i} M(x) = 0$), so the evolution equation becomes

$$dX_t^\varepsilon = -M(X_t^\varepsilon) \nabla U(X_t^\varepsilon) dt + \sqrt{\varepsilon} M^{1/2}(X_t^\varepsilon) dW_t, \quad (25)$$

where $M^{1/2}(M^{1/2})^T = M$. Then it still holds that $\frac{1}{2}V(x) = U(x) = S(x)$, and Lagrangian and Hamiltonian of equation (23) are modified by choosing the

appropriate inner products $\langle u, v \rangle_M = \langle u, M^{-1}v \rangle$ and $|u|_M = \langle u, u \rangle_M^{1/2}$, with

$$L(\psi, \dot{\psi}) = \frac{1}{2} |\dot{\psi} + M(\psi) \nabla U(\psi)|_M^2,$$

$$H(\psi, \theta) = -\langle \theta, M(\psi) \nabla U \rangle + \frac{1}{2} |M(\psi) \theta|_M^2.$$

In this case, the minimizer obeys the modified relation

$$\dot{\phi} = \pm M(\phi) \nabla U(\phi), \quad (26)$$

and the reversibility condition $H(\psi, \nabla U - \theta) = H(\psi, \nabla U + \theta)$ is fulfilled. Equations (25) and (26) are still within the realm of classical gradient flows (with mobility). In the next section we will encounter examples that cannot be phrased even in this form, in general because the associated Hamiltonian is non-quadratic, corresponding to a non-Gaussian large deviation principle.

Remark 3. If $M(x)$ is not divergence free, the reversibility condition is still applicable if equation (25) additionally is extended by the deterministic drift $\varepsilon \operatorname{div} M(x) dt$, while the LDP remains unchanged [23].

Remark 4. If $M(x)$ is not symmetric, the reversibility condition is violated. In this case though, the adjoint dynamics can be written down explicitly. Decompose $M = S + A$, with $S = S^T$ and $A = -A^T$. Then the adjoint dynamics are

$$dX_t^\varepsilon = -(S - A) \nabla U(X_t^\varepsilon) dt + \sqrt{\varepsilon} S^{1/2} dW_t,$$

and a modified string method can be built. This is a special case of the traverse decomposition [6, Chpt 4, Thm 3.1].

B. Chemical Reaction Network

In the context of chemical reactions and birth-death processes, one considers networks of several reactants in a container of volume D which is well-stirred. Take for example the reaction network



where each process is Poisson with rates $k_i > 0$, and where the concentrations of the reactants A and B are held constant. This system was introduced in [24]. Even though it can be considered unrealistic for practical purposes, in particular because of the presence of ternary reactions, it serves as a toy model to understand bi-stable reaction networks. Its dynamics can be modeled as a MJP on \mathbb{Z}_+ with generator

$$(\mathcal{L}f)(n) = A(n) (f(n+1) - f(n)) + B(n) (f(n-1) - f(n)) \quad (27)$$

and with the propensity functions

$$\begin{aligned} A(n) &= k_0 D + (k_2/D) n(n-1) \\ B(n) &= k_1 n + (k_3/D^2) n(n-1)(n-2). \end{aligned}$$

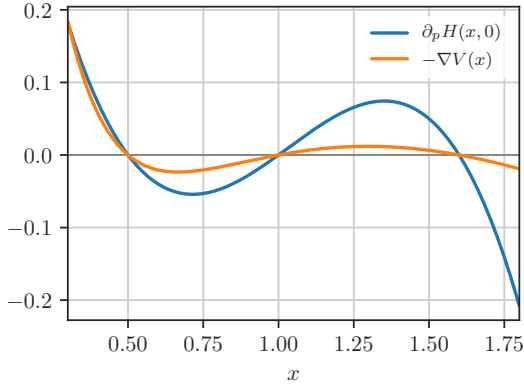


Figure 1: Plot of $\partial_p H(x, 0)$ (blue line) and $-\nabla V(x)$ (orange line) versus x . The x-axis ranges from 0 to 1.75, and the y-axis ranges from -0.2 to 0.2. Both curves start at approximately 0.18 at $x=0$, cross the zero line at $x \approx 0.4$, reach a minimum of about -0.05 at $x \approx 0.75$, and then oscillate around zero with a local maximum of about 0.08 at $x \approx 1.35$.

$\partial_p H(x, 0) =$

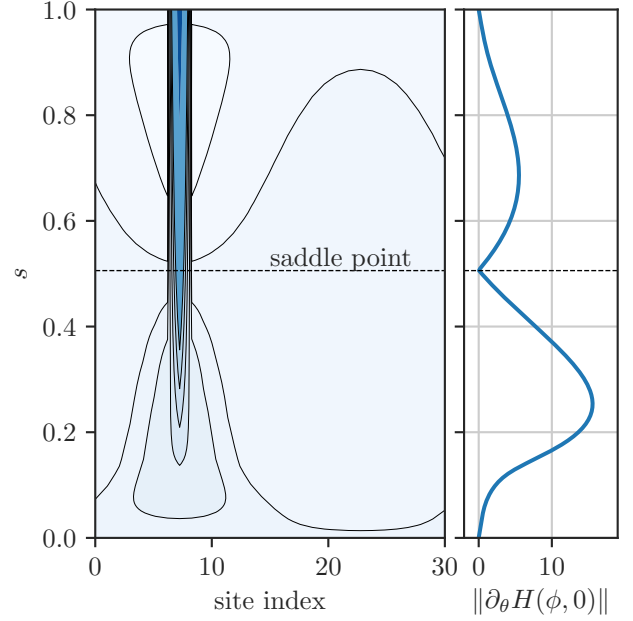


Figure 2: Plot of $\|\partial_\theta H(\phi, 0)\|$ (blue line) versus site index. The x-axis ranges from 0 to 30, and the y-axis ranges from 0.0 to 1.0. The plot shows a sharp peak at site index ≈ 7 and a sharp valley at site index ≈ 25 . A dashed horizontal line at $s \approx 0.5$ is labeled 'saddle point'.

The model above satisfies a large deviation principle in the following scaling limit: Denote by $c = n/D$ the concentration of X , and normalize it by a typical concentration c_0 , so that $x = c/c_0$. Now, for a large number of particles per lattice site $c_0 D = \epsilon^{-1}$, we obtain to leading order

$$(\mathcal{L}^\epsilon f)(x) = \epsilon^{-1} \left(a(x) (f(x + \epsilon) - f(x)) + b(x) (f(x - \epsilon) - f(x)) \right), \quad (28)$$

on $\mathcal{E}^\epsilon = \epsilon \mathbb{Z}_+$, where we defined $k_i = \lambda_i (c_0)^{1-i}$, and

$$a(x) = \lambda_0 + \lambda_2 x^2, \quad b(x) = \lambda_1 x + \lambda_3 x^3.$$

The large deviation principle for (28) can be formally obtained via WKB analysis which gives a Hamilton-Jacobi operator associated with a Hamiltonian that is also the one rigorously derived in LDT [25],

$$H(x, p) = a(x) (e^p - 1) + b(x) (e^{-p} - 1).$$

Note that this Hamiltonian is not quadratic in its conjugate momentum, implying that no Gaussian SDE exists (including no diffusion in a potential) with the same large deviation principle. Detailed balance is nevertheless fulfilled, by realizing that

$$\nabla V(x) = \log \frac{b(x)}{a(x)}, \quad (29)$$

under which the reversibility condition $H(x, p) = H(x, \nabla V - p)$ is confirmed. The large deviation minimizers can therefore explicitly be computed to be

$$\dot{x} = \pm \partial_p H(x, 0) = \pm (a(x) - b(x)).$$

This precisely corresponds to the law of mass-action of the reaction network, as well as its time-reversed variant.

The generalized gradient flow for this system is explicitly given by

$$\dot{x} = \partial_p \psi_x^* (-\nabla S),$$

with $\nabla S = \frac{1}{2} \nabla V$ given by (29) and

$$\psi_x^*(p) = \sqrt{ab} (e^p - 1) + \sqrt{ab} (e^{-p} - 1).$$

Figure 2 highlights the fact that these dynamics are very different from the gradient of the potential itself: Even though both disappear at the fixed points, their behavior away from the fixed points does not agree.

C. Zero-range process

Consider a lattice gas on a one dimensional lattice with $L \in \mathbb{N}$ sites, where on each lattice site i there are n_i particles. The system state is described by $\vec{n} \in \mathbb{Z}_+^L$. Particles can hop to neighboring sites on the left or right with a rate $\gamma(n_i)$ depending only on the local occupation number, so that the total number of particles N is conserved, $N = \sum_{i=1}^L n_i$. Such a system is called a zero-range process (ZRP), which is a MJP with generator

$$\mathcal{L}f(\vec{n}) = \sum_{i=1}^L \gamma(n_i) (f(\vec{n} + \vec{e}_i^+) + f(\vec{n} + \vec{e}_i^-) - 2f(\vec{n})),$$

where \vec{e}_i^\pm is the vector with zero entries everywhere, except -1 at i and 1 at $i \pm 1$. For finite L , a large deviation principle can be obtained for this MJP in $\varepsilon = N^{-1} \rightarrow 0$ by considering the rescaled quantity $\rho_i = \bar{\rho} n_i / N = \varepsilon n_i$, $\bar{\rho} > 0$, for $\mathcal{E}^\varepsilon = \varepsilon \mathbb{Z}_+^L$ and $\mathcal{E} = \mathbb{R}_+^L$. After furthermore rescaling time, the generator then reads

$$\mathcal{L}^\varepsilon f(\vec{\rho}) = \varepsilon^{-1} \sum_{i=1}^L \gamma(\rho_i) (f(\vec{\rho} + \varepsilon \vec{e}_i^+) + f(\vec{\rho} + \varepsilon \vec{e}_i^-) - 2f(\vec{\rho})) ,$$

where the jump rates γ have been rescaled appropriately [5, 15]. The large deviation Hamiltonian reads

$$H(\rho, \theta) = \sum_i \gamma(\rho_i) (e^{\theta_{i-1} - \theta_i} + e^{\theta_{i+1} - \theta_i} - 2) . \quad (30)$$

Note again that the Hamiltonian is non-quadratic in the conjugate momentum, meaning that no Gaussian SDE can be found with large deviation Hamiltonian (30). The system is not in detailed balance in general, but one can choose the rates $\gamma(x)$ in order to enforce reversibility. The reversibility condition amounts to

$$\frac{P(\vec{\rho} \rightarrow \vec{\rho} + \varepsilon \vec{e}_i^+)}{P(\vec{\rho} + \varepsilon \vec{e}_i^+ \rightarrow \vec{\rho})} = \frac{\rho_\infty(\vec{\rho} + \varepsilon \vec{e}_i^+)}{\rho_\infty(\vec{\rho})} \quad (31)$$

i.e. the ratio of forward and backward reaction rates has to correspond to the relative probability of the respective states. Since the density ρ_∞ is connected to the quasipotential via $\rho_\infty(\vec{\rho}) \asymp \exp(-\varepsilon^{-1} V(\vec{\rho}))$ as per section III A, and furthermore $P(\vec{\rho} \rightarrow \vec{\rho} + \varepsilon \vec{e}_i^+) = \gamma(\rho_i)$, and $P(\vec{\rho} + \varepsilon \vec{e}_i^+ \rightarrow \vec{\rho}) = \gamma(\rho_{i+1})$, the reversibility condition (31) for $\varepsilon \rightarrow 0$ translates to

$$\frac{\gamma(\rho_{i+1})}{\gamma(\rho_i)} = \exp(-(\nabla_i V(\vec{\rho}) - \nabla_{i+1} V(\vec{\rho}))) .$$

A possible choice to fulfill this constraint is

$$\nabla_i V(\vec{\rho}) = \ln \gamma(\rho_i) + C , \quad (32)$$

where the constant C is fixed by the conserved mean density $\bar{\rho} = L^{-1} \sum_i \rho_i$ via $C = -\ln \gamma(\bar{\rho})$. We therefore obtain

$$V(\vec{\rho}) = \sum_i \int_0^{\rho_i} (\ln \gamma(y) + C) dy ,$$

which is the correct potential for the ZRP [26]. In particular, for non-interacting particles, we have $\gamma(x) = x$ and

$$V(\vec{\rho}) = \sum_i \rho_i \ln \left(\frac{\rho_i}{\bar{\rho}} \right) - \rho_i .$$

For general $\gamma(x)$ obeying the reversibility condition, the transition trajectories now follow

$$\dot{\rho}_i = \pm \partial_{\theta_i} H(\vec{\rho}, 0) = \pm (\gamma(\rho_{i-1}) + \gamma(\rho_{i+1}) - 2\gamma(\rho_i)) . \quad (33)$$

To highlight that this flow again is a generalized gradient flow, note that (33) is of the form

$$\dot{\rho}_i = \partial_{\theta_i} \psi_\rho^* (-\nabla S(\vec{\rho})) ,$$

with $\nabla S(\rho) = \frac{1}{2} \nabla V(\rho)$ given by (32) and

$$\begin{aligned} \psi_\rho^*(\vec{\theta}) &= \sum_i \sqrt{\gamma_i \gamma_{i-1}} (e^{\theta_{i-1} - \theta_i} - 1) \\ &+ \sum_i \sqrt{\gamma_i \gamma_{i+1}} (e^{\theta_{i+1} - \theta_i} - 1) , \end{aligned}$$

where $\gamma_i = \gamma(\rho_i)$.

Notably, for specific choices of $\gamma(x)$, this system has multiple stable fixed points. For example, taking $\gamma(x) = D + \exp(-x)$, for $D = \frac{1}{10}$ and $\bar{\rho} = 1$ provides two stable fixed points, one being a constant solution at $\rho_i = \bar{\rho}$ and one being a *condensate*, where a macroscopic fraction of the density is concentrated in a single lattice site. This setup is metastable in that fluctuations from the finiteness of the number of particles will eventually force the system from one fixed-point to the other, the transition happening along the heteroclinic orbits of equation (33) in the limit $N \rightarrow \infty$. The corresponding transition trajectory is depicted in figure 3 (left). Here, the x -axis represents the site index, in this particular case from 0 to 30 with $L = 31$. The y -axis represents the parameter s along the string. The shading of the contour plot depicts each configuration $\vec{\rho}(s)$ along the string, starting at the constant density at $s = 0$, and transitioning into the condensate at $s = 1$. The relevant saddle is reached at $s = 0.5$, marked as a dashed line in the contour plot, and identified through the point at which $\|\partial_\theta H(\phi, 0)\| = 0$, depicted in figure 3 (right). Notably, a spatially extended condensate forms into a *critical nucleus*, which is reached at the saddle point.

D. Interacting particle system

On a periodic domain $\Omega = [0, 1]$, consider a system of N interacting Brownian particles at $X_i \in \Omega$, $i \in \{1, \dots, N\}$, in a potential $U(x) : \Omega \rightarrow \mathbb{R}$ and with interaction potential $K(x)$. Each particle is modeled by its own Itô diffusion,

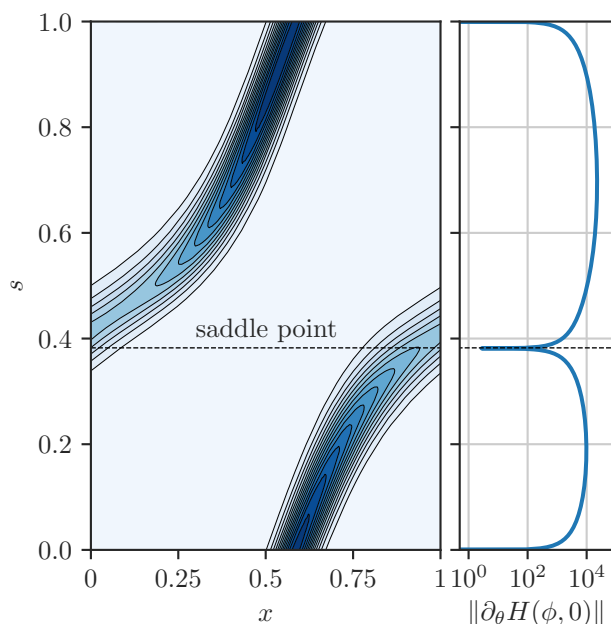
$$\begin{aligned} dX_i(t) &= -\nabla U(X_i(t)) dt \\ &- \frac{1}{N} \sum_{j=1}^N \nabla K(X_i(t) - X_j(t)) dt + \sqrt{2} dW_i(t) . \end{aligned}$$

The hydrodynamic limit of this system is

$$\partial_t \rho = \partial_x^2 \rho + \partial_x (\rho \partial_x U + \partial_x (\rho \star K)) .$$

As discussed in [27], this can be interpreted as a generalized gradient flow in the (ρ -dependent) Wasserstein metric, evolving according to

$$\partial_t \rho = -M(\rho) \nabla_\rho V, \quad M(\rho) \xi = -\nabla \cdot (\rho \nabla \xi)$$



tial is not symmetric, resulting in an effective net force, e.g. to the right for $\delta > 0$. In total, particles tend to stick together and try to move right, but collect within the basin of the potential. As a consequence, the system is not meta-stable, and the unique fixed point is a cluster of particles slightly off $x = \frac{1}{2}$. We can nevertheless compute an interesting transition trajectory: We can force the particle cloud to revolve once around the periodic domain, i.e. ask for the most likely trajectory that leads to the particles collectively traveling up the barrier of $U(x)$ towards $x = 1$, and down again from $x = 0$ towards the fixed point. The resulting string is depicted in figure 4 (left). Again, the contour plot represents the configurations $\rho(x)$ along the string parameter $s \in [0, 1]$, starting and ending at the same (fixed point) configuration, but wrapping around the periodic domain once. The corresponding strength of the gradient drift is depicted in figure 4 (right), which identifies the relevant saddle for the transition. Concretely, we choose $\alpha = 0.5 \cdot 10^3$, $\beta = 0.5 \cdot 10^2$, and $\delta = 5 \cdot 10^{-2}$.

VII. CONCLUDING REMARKS

In this paper, we showed how the fact that a large deviation principle induces a generalized gradient flow for reversible processes can be used to obtain geometric properties of limiting transition trajectories between fixed points. In particular, we showed that under suitable conditions every minimizer of a large deviation principle of a reversible process can be interpreted as a heteroclinic orbit (or its time-reverse) in a generalized gradient flow.

This fact has important consequences for the numerical computation of the most likely transition trajectories. In particular, the string method, originally devised to effectively compute minimizing trajectories for diffusions in a potential landscape, can be adapted to the wider class of generalized gradient flows.

We demonstrated the feasibility of this approach by computing transition trajectories for the condensation of a zero range process, a particular lattice gas model, as well as the hydrodynamic limit of interacting particles, in all cases computing the most likely trajectory realizing a certain event, and identifying the saddle point along the transition, at which the dynamics cross between the different basins of attraction.

ACKNOWLEDGMENTS

TG would like to thank M. Peletier, A. Montefusco, E. Vanden-Eijnden, and H. Touchette for fruitful discussions.

$\rho(s, x)$

$s \in [0, 1]$

with

$$V(\rho) = \int \left(\rho \log \rho - \rho + \rho U + \frac{1}{2} \rho (K \star \rho) \right) dx.$$

On the other hand, from a large deviation perspective, the Hamiltonian of this system reads

$$\begin{aligned}
 H(\rho, \theta) &= \int_0^1 (\theta \partial_x^2 \rho + \theta \partial_x (\rho \partial_x U + \partial_x (\rho \star K)) - \rho (\partial_x \theta)^2) dx \\
 &= \langle -M(\rho) \nabla_\rho V(\rho), \theta \rangle + \langle \theta, M(\rho) \theta \rangle,
 \end{aligned}$$

where the inner product and norm are L^2 . As concrete demonstration of our algorithm, we take a periodic potential $U(x) = \alpha \cos(2\pi x)$, which has a unique minimum at the center of the domain. As interaction potential, we pick $K(x)$ such that $\partial_x K(x) = w(x - \delta)$, with

$$w(x) = \begin{cases} \beta x \exp\left(-\frac{2x^2}{1-2x^2}\right) & x \leq \frac{1}{2} \\ 0 & \text{else,} \end{cases}$$

which results in a locally parabolic interaction which tapers off to 0. Notably, for $\delta \neq 0$, the interaction poten-

- Journal of Physical Chemistry B 109 850
- Hydrodynamic fluctuations in fluids and fluid mixtures
- Reviews of Modern Physics 87 8
- Random perturbations of dynamical systems
- Physical Review B 66 0
- J. Chem. Phys. 126 0
- SIAM Journal on Mathematical Analysis
- Potential Analysis 41 900
- Journal of Physics: Condensed Matter 21 06
- Journal of Statistical Physics 145 880
- Stochastic Analysis and Applications 25 150
- The Annals of Applied Probability 26
- Large deviations for stochastic processes (Mathematical surveys and monographs)
- Fluctuations and Stochastic Phenomena in Condensed Matter
- Physics Reports 478 06
- Journal of Statistical Physics 170 06
- SIAM Journal on Scientific Computing 26 30
- Communications on Pure and Applied Mathematics 61 0
- Recent Progress and Modern Challenges in Applied Mathematics, Modeling and Computational Science
- Annual Review of Physical Chemistry 59 050
- The Journal of Chemical Physics 140 30
- Zeitschrift für Physik 253 05
- Large Deviations For Performance Analysis: Queues, Communication and Computing
- Journal of Statistical Physics 113 06
- Philosophical Transactions of the Royal Society of London Series A 371 06